BIOCHEMISTRY
including biophysical chemistry & molecular biology

Article

pubs.acs.org/biochemistry

Two Translation Products of *Yersinia yscQ* Assemble To Form a Complex Essential to Type III Secretion

Krzysztof P. Bzymek,[†] Brent Y. Hamaoka, and Partho Ghosh*

Department of Chemistry and Biochemistry, 9500 Gilman Drive, University of California, San Diego, La Jolla, California 92093-0375, United States

Supporting Information

ABSTRACT: The bacterial flagellar C-ring is composed of two essential proteins, FliM and FliN. The smaller protein, FliN, is similar to the C-terminus of the larger protein, FliM, both being composed of SpoA domains. While bacterial type III secretion (T3S) systems encode many proteins in common with the flagellum, they mostly have a single protein in place of FliM and FliN. This protein resembles FliM at its N-terminus and is as large as FliM but is more like FliN at its C-terminal SpoA domain. We have discovered that a FliN-sized cognate indeed exists in the *Yersinia* T3S system to accompany the FliM-sized cognate. The FliN-sized cognate, YscQ-C, is the product of an internal translation initiation site within the locus encoding the FliM-sized cognate YscQ. Both intact YscQ and YscQ-C were found to be required for T3S, indicating that the internal translation initiation site, which is conserved in some but not all YscQ orthologs, is crucial for function. The crystal structure of YscQ-C revealed a SpoA domain that forms a highly intertwined, domain-swapped homodimer, similar to those observed in FliN and the YscQ ortholog $HrcQ_B$. A single YscQ-C homodimer associated reversibly with a single molecule of intact YscQ, indicating conformational differences between the SpoA domains of intact YscQ and YscQ-C. A "snap-back" mechanism suggested by the structure can account for this. The 1:2 YscQ–YscQ-C complex is a close mimic of the 1:4 FliM–FliN complex and the likely building block of the putative *Yersinia* T3S system C-ring.

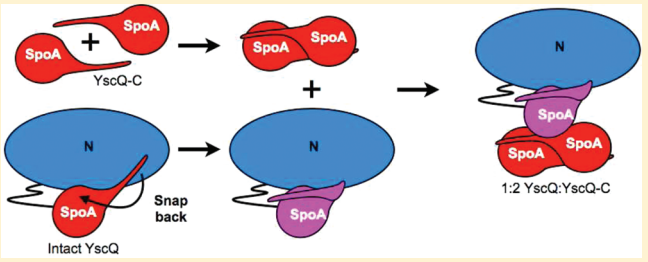

The type III secretion (T3S) system is essential to the pathogenesis of numerous Gram-negative bacteria.[1,2] This system transports select bacterial proteins, many of them virulence factors, into host cells. The transport is presumed to occur directly from the bacterial cytosol through a hollow needle,[3] although an indirect route also appears to exist.[4] The precise means by which proteins are recognized within the bacterium for transport is not understood. Among candidate recognition factors are T3S proteins related to proteins of the bacterial flagellar C-ring,[5,6] which is the most cytoplasmically disposed of the flagellar rings and which plays a role in both protein transport and flagellar rotation.[7] The flagellar C-ring is composed of two proteins, FliM (38 kDa) and FliN (15 kDa), which are related. FliN is similar in sequence to the C-terminus of FliM, both being composed of SpoA domains that mediate the formation of a FliM–FliN complex.[8−10] In *Escherichia coli*, these complexes have been determined to have a 1:4 FliM:FliN stoichiometry,[8] and in *Salmonella*, ∼32−36 FliM–FliN complexes have been estimated to form the C-ring.[6]

While the T3S system version of the C-ring has not yet been visualized,[11,12] most T3S systems encode a single protein in place of FliM and FliN that has been found to be essential for T3S.[13−16] This protein resembles FliM at its N-terminus and is as large as FliM, but is more like FliN at its C-terminal SpoA domain. Most T3S systems appear to lack the smaller FliN-sized cognate to accompany the FliM-sized cognate. This is the case for *Yersinia* spp., which encode the FliM-sized cognate YscQ (34 kDa) but appear to lack the FliN-sized cognate. YscQ is essential for T3S and interacts with a number of components of the T3S apparatus.[11,13,17,18] A complex containing YscQ, YscN (the T3S ATPase), YscL (negative regulator of YscN), and YscK (undefined function) appears to coassemble during formation of the T3S apparatus.[11] YscQ is also reported to interact with YscP, a regulator of needle length.[19] Except for the association with the needle length regulator, these interactions are conserved in the YscQ orthologs *Shigella* Spa33,[12] *Salmonella* SpaO,[14] and *E. coli* EscQ (SepQ).[15] In addition, the *Chlamydia* ortholog CdsQ has been reported to interact with the ortholog of YscL, CdsL, and the ortholog of the structural protein YscD, CdsD.[20] Spa33 and SpaO along with *CdsQ*[21] have also been shown to associate with transported proteins, suggesting that these YscQ orthologs help in the recognition of T3S-transported substrates.[12] Both CdsQ and SpaO further interact with T3S chaperones,[14,21] which associate with certain transported proteins and are required for the transport of these proteins. In the case of SpaO, evidence that it acts as a sorting platform exists, such that the interactions with transported proteins are made in sequential order.[14]

Received: December 6, 2011
Revised: February 7, 2012
Published: February 9, 2012

To understand the nature of the putative C-ring in the *Yersinia* T3S system, we isolated YscQ from *Yersinia pseudotuberculosis* and found that it exists as a complex composed of intact YscQ and a C-terminal fragment of YscQ that closely corresponds to FliN in size and sequence. We found that the C-terminal fragment, called YscQ-C, is a product of an internal translation initiation site, which is conserved in some but not all YscQ family members. This is similar to the recent discovery that in the *Salmonella* SPI-2 T3S system, the YscQ ortholog SsaQ is produced also as an intact protein and a C-terminal fragment because of an internal translation start site.[16] However, unlike the case for SsaQ in which the C-terminal fragment is dispensable for T3S, YscQ-C was found to be required for T3S. The crystal structure of YscQ-C was determined, showing that it consists of a SpoA domain that forms a highly intertwined, domain-swapped homodimer, resembling the structures of fragments of *Thermotoga maritima* FliN[8] and the *Pseudomonas syringae* ortholog of YscQ, $HrcQ_B$.[22] We found that a single homodimer of YscQ-C associated with a single monomer of intact YscQ, indicating conformational differences between the SpoA domains of intact YscQ and YscQ-C. We propose a "snap-back" mechanism suggested by the structure to account for this difference. The 1:2 YscQ–YscQ-C complex is a close mimic of the 1:4 FliM–FliN complex and the likely building block of the putative T3S C-ring in *Yersinia*.

EXPERIMENTAL PROCEDURES

DNA Constructs and Mutagenesis. The coding sequence for YscQ (residues 1–307, with an S2G substitution to accommodate a DNA restriction site) and YscQ-C (residues 218–307, with an S219G substitution to accommodate a DNA restriction site) was amplified by polymerase chain reaction (PCR) from the pYV plasmid of *Y. pseudotuberculosis* 126[23] and used for generation of pET28b(+) (EMD, San Diego, CA) and, in the case of YscQ, also pBAD-A (Invitrogen, Carlsbad, CA) expression constructs. A PreScission protease cleavable C-terminal histidine tag was added to YscQ and YscQ-C in all pET28b(+) constructs, and to YscQ in some pBAD constructs. YscQ(M218A) was expressed with a noncleavable His tag. Mutagenesis to generate YscQ(M218A) and other mutant proteins was performed using the QuikChange mutagenesis kit (Agilent). The integrity of all constructs was verified by DNA sequencing.

Protein Expression in *E. coli* and Purification. Wild-type YscQ and YscQ(M218A) were expressed using pET28b(+) in *E. coli* BL21(DE3). Bacteria were grown at 37 °C in LB medium containing kanamycin (100 μg/mL) to an OD_{600} of 0.8–1.2, cooled to 18 °C for the induction of protein expression through the addition of 0.5 mM isopropyl β-D-thiogalactoside, and then grown further at 18 °C overnight. Identical procedures were followed for expression of YscQ-C, except that the temperature was maintained at 37 °C and bacteria were grown for only 3 h following induction. Bacteria were pelleted by centrifugation (10 min at 8000*g* and 4 °C), and the pellet was resuspended in 150 mM NaCl, 50 mM Tris (pH 8.0) (TBS), and 1 mM phenylmethanesulfonyl fluoride (5 mL/g of wet cell paste). Bacteria were lysed using an EmulsiFlex-C5 (Avestin); cell debris was pelleted by centrifugation (30 min at 20000*g* and 4 °C), and the supernatant was applied to a Ni^{2+}-nitrilotriacetic acid (NTA) column (Sigma). Following being extensively washed with TBS containing 5 mM imidazole, bound protein was eluted in TBS containing 250 mM imidazole. Eluted fractions were dialyzed or buffer exchanged by diafiltration [Amicon YM10 for YscQ and YscQ(M218A) or YM3 for YscQ-C] into TBS. For constructs with a cleavable His tag, His-tagged PreScission protease was added at a 1:100 protease:substrate mass ratio and the mixture incubated overnight at 4 °C. The sample was then reapplied to a Ni^{2+}-NTA column, and cleaved YscQ was collected in the flow-through fractions. YscQ constructs were further purified on a Superdex 200 column (GE Healthcare) and concentrated to 6–15 mg/mL for storage at −80 °C. The concentration of YscQ constructs was determined using calculated molar absorption coefficients. For phasing purposes, the methionine substitution mutant YscQ-C(I248M) was constructed. Selenomethionine (SeMet)-substituted YscQ-C(I248M) was prepared as previously described[24] and purified as described above, except that 5 mM 2-mercaptoethanol (2-ME) was included in all buffers.

N-Terminal Sequencing. N-Terminal amino acid sequencing was conducted at the University of California, San Diego, Division of Biological Sciences Protein Sequencing Facility.

Static Light Scattering. Absolute molecular masses were determined by multiangle static light scattering (SLS). Protein samples in 150 mM NaCl, 50 mM Tris, or HEPES (pH 7.4) were applied to a TSK-Gel G4000 WXL size-exclusion column (Tosoh, Bioscience) attached to a miniDAWN TREOS SLS detector and an Optilab T-rEX refractive index detector (Wyatt, Santa Barbara, CA). Data were processed using ASTRA version 5 (Wyatt).

Protein Crystallization. YscQ-C at 4–16 mg/mL in 10 mM Tris (pH 8.0) was crystallized by the vapor diffusion hanging drop method using 1.4–1.55 M $(NH_4)_2SO_4$ and 100 mM Tris (pH 7.8–8.8) as the precipitant at a 1:1 protein:precipitant ratio. SeMet-substituted YscQ-C(I248M) at 7.75 mg/mL in 10 mM Tris (pH 8.0) and 5 mM 2-ME was crystallized by the sitting drop vapor diffusion method with an Oryx6 crystallization robot (Douglas Instruments) using 100 mM Tris (pH 7.4–8.2), 40–120 mM $MgCl_2$, and 3–12% PEG 400 as the precipitant at 3:7 and 6:4 protein:precipitant ratios.

Structure Determination. Crystals of YscQ-C and YscQ-C(I248M) were cryoprotected using a 1:2 (v:v) paratoneN:paraffin ratio and cooled in liquid nitrogen. Diffraction data for crystals of YscQ-C were collected on APS beamline 23 ID-B (Argonne National Laboratory, Argonne, IL), as were single-wavelength anomalous dispersion (SAD) data for crystals of SeMet-substituted YscQ-C(I248M). Diffraction data for YscQ-C and YscQ-C(I248M) were processed using XDS[25] and HKL2000,[26] respectively. Phases were calculated and refined using the programs Phaser and Resolve within Phenix.[27] Two SeMet positions were identified in the asymmetric unit, which contains a dimer of YscQ-C. Automated model building using Phenix resulted in an initial model that contained 143 of the 172 residues in the final model. The initial model was manually modified using Coot through inspection of σ_A-weighted $2mF_o - DF_c$ and $mF_o - DF_c$ maps,[28] followed by cycles of refinement using Phenix. Default parameters and target weights defined by Phenix were used (three macro cycles of bulk solvent correction and anisotropic scaling and up to 25 iterations of coordinate, atomic displacement parameters and occupancy refinement). The model was verified by inspection of composite omit maps calculated using CNS (5% of the model omitted, σ_A-weighted $2mF_o - DF_c$ maps).[29] Waters were added in later stages of the refinement using Phenix with default parameters (3σ peak height in $mF_o - DF_c$ maps),

followed by inspection of maps. Continuous electron density for the main chain was evident for residues 229−313 of chain A and residues 228−313 of chain B, and all side chains were in electron density, except for Q291 of chain A and Q239 of chain B.

The structure of native, wild-type YscQ-C was determined by molecular replacement with Molrep using YscQ-C-(Ile248SeMet) as the search model.[30] The same refinement protocol described above was used, except that Cartesian simulated annealing was conducted in Phenix (using default parameters) in the first round of refinement. TLS refinement was performed in the final stages of structure refinement with 12 TLS groups (for chain A, residues 229−244, 245−250, 251−265, 266−271, 272−279, 280−290, 291−301, and 302−313; for chain B, residues 229−239, 240−271, 272−301, and 302−313).[31] Continuous electron density was observed for residues 229−313 of both chains. All side chains were in electron density with the exception of Q239 and Q291 of chain A and Q239 of chain B. The final map had correlation coefficients of 0.90 and 0.75 for the main and side chains, respectively, as calculated with OVERLAPMAN.[30] The overall Molprobity score was 1.68, corresponding to the 97th percentile.[32] Data collection and model statistics are listed in Table 1.

Table 1. Data Collection and Refinement Statistics

	YscQ-C	SeMet YscQ-C(I248M)
	Data Collection	
λ (Å)	0.96860	0.97948
resolution (Å)[a]	34.42−2.25 (2.31−2.25)	50−2.16 (2.20−2.16)
space group	*H*32	*H*32
cell dimensions (Å)	$a = b = 114.1$, $c = 88.6$	$a = b = 114.2$, $c = 91.5$
no. of unique reflections	10594	12457
avg multiplicity[a]	10.8 (9.8)	17.7 (3.6)
I/σ_I[a]	32.1 (10.5)	32.4 (2.1)
completeness (%)[a]	99.3 (94.2)	97.4 (76.2)
R_{merge} (%)[a]	4.7 (23.2)	8.3 (53.9)
	Refinement	
resolution (Å)[a]	34.42−2.25 (2.48−2.25)	
no. of reflections	10592	
no. of atoms		
protein	1370	
solvent	50	
R_{work}/R_{free} (%)[a]	20.2/23.3 (26.6/32.4)	
rmsd		
bond lengths (Å)	0.009	
bond angles (deg)	1.244	
average *B* factor (Å^2)		
protein	47.6	
solvent	48.5	
Ramachandran (%)[b]		
favored	98.8	
allowed	1.2	
disallowed	0	

[a]Data for the highest-resolution shell in parentheses. [b]Structure validation by Molprobity.[32]

Molecular figures were made with PyMol (http://pymol.sourceforge.net). Structure-based sequence alignments were generated using Expresso[33] and displayed using ESPript.[34] The crystal structure and structure factors have been deposited in the Protein Data Bank as entry 3UEP.

Deletion of *yscQ* in *Y. pseudotuberculosis*. To generate *Y. pseudotuberculosis* (Δ*yscQ*), the entirety of *yscQ*, except for 22 bp at the 3′ end that contains a ribosome-binding site for *yscR*, was substituted in-frame with *aph* (kanamycin resistance) by homologous recombination using a PCR fragment, as described previously.[35,36] The PCR fragment (1799 bp) consisted of 504 bp of pYV sequence upstream of *yscQ*, followed by *aph*, the 22 bp from the 3′ end of *yscQ*, and 479 bp of pYV sequence downstream of *yscQ*. A minor modification was made to the published protocol to increase the induction time for expression of the λ red recombinase proteins. The proper substitution of *yscQ* with *aph* was verified by DNA sequencing.

Allelic Replacement of *yscQ*. Replacement of *aph* with *yscQ* alleles in *Y. pseudotuberculosis* (Δ*yscQ*) through homologous recombination was conducted using plasmid pSB890,[37] as previously described with some modifications.[38] Plasmid pWL204, which carries the λ red recombinase genes, was first transformed into *Y. pseudotuberculosis* (Δ*yscQ*) to facilitate recombination.[35] This was followed by transformation of plasmid pSB890 carrying mutant *yscQ* alleles flanked by 504 and 457 bp of pYV sequence upstream and downstream, respectively, of *yscQ*. In addition, insertion of pSB890 into pYV was selected for by growth on agar plates containing tetracycline followed by growth in liquid medium (BHI) containing tetracycline. The proper replacement of *aph* with *yscQ* alleles was verified by DNA sequencing.

Secretion Assay. Type III secretion was examined as previously published.[38] Briefly, *Y. pseudotuberculosis* strains expressing *yscQ* from its native locus on the pYV plasmid were induced for type III secretion for 3 h in Ca^{2+}-deficient medium at 37 °C, whereupon the medium was separated from bacteria by centrifugation (5 min at 14000*g* and 23 °C), and the medium was precipitated with trichloroacetic acid (TCA) and resolubilized for analysis by Coomassie-stained sodium dodecyl sulfate−polyacrylamide gel electrophoresis (SDS−PAGE). Prior to centrifugation of bacteria, the OD_{600} of samples was measured for normalization. An identical procedure was followed for *Y. pseudotuberculosis* (Δ*yscQ*) complemented with pBAD containing wild-type or variant YscQ, except that 0.1% L-arabinose was included in the growth medium before the induction of secretion. Immediately prior to the induction of secretion, fresh L-arabinose was added to a final concentration of 0.2%.

Detection of YscQ in *Y. pseudotuberculosis*. Rabbit anti-YscQ polyclonal antibodies raised against YscQ-C as an antigen (Abgent, San Diego, CA) were purified using a YscQ-C affinity column (cross-linked to Aminolink resin, Pierce, Rockford, IL) and used as the primary antibody in Western blots or cross-linked to Aminolink resin for isolation of YscQ from *Y. pseudotuberculosis*. For the latter, *Y. pseudotuberculosis* was grown under nonsecreting conditions (BHI containing 2 mM $CaCl_2$ at 28 °C) to an OD_{600} 0.64−0.66, at which point EGTA and $MgCl_2$ were added to a final concentration of 10 mM each, and the culture was shifted to 37 °C to induce secretion and grown further for 3 h. Bacteria were harvested by centrifugation, resuspended in PBS, and lysed by being passed three times through an EmulsiFlex-C5 (Avestin), and cell debris was removed by centrifugation (30 min at 20000*g* and 4

°C). The supernatant was then applied to the anti-YscQ-C antibody column, which was then washed extensively with PBS, and bound proteins were eluted with 0.1 M glycine (pH 2.9) and immediately neutralized with 1 M Tris (pH 9.0). The eluate was concentrated in a SpeedVac or precipitated with TCA prior to Western blot analysis.

Western Blot. Samples were separated via 12% SDS−PAGE and transferred to a PVDF membrane using a Trans-Blot semi dry cell (Bio-Rad, Hercules, CA) for 25−30 min at 15−30 V. The membrane was blocked overnight at 4 °C in 5% nonfat dry milk in PBST (PBS including 0.1% Tween 80), washed once with PBST, and incubated for 1 h at 23 °C with a primary antibody [1:2000 anti-His (Santa Cruz Biotechnology, Santa Cruz, CA) or 1:1000 purified anti-YscQ-C] in 5% nonfat dry milk in PBST, followed by three washes with PBST. An HRP-conjugated secondary antibody (Santa Cruz Biotechnology) at a 1:10000 dilution was incubated with the membrane in 5% nonfat dry milk. Following extensive washes with PBST, the membrane was developed using an ECL Western Blotting system (GE Healthcare, Piscataway, NJ) and visualized with Amersham Hyperfilm ECL (GE Healthcare).

Ni^{2+}-NTA Coprecipitation. Proteins were incubated overnight at 4 °C in 100 μL of PBS at 40 μM, except for the high-concentration sample of YscQ-C-His_6, which was at 280 μM. Samples were then centrifuged (10 min at 15800*g* and 4 °C). Ten microliters was reserved as the input sample. Eighty microliters of the sample was then incubated for 30 min at 4 °C with end-over-end agitation with 50 μL of an ∼50% HIS-select Ni^{2+} affinity gel (Sigma) slurry, which had been washed with PBS. The resin was washed five times with 1 mL of 500 mM NaCl, 20 mM Tris (pH 8), 40 mM imidazole, and 0.1% Triton X-100, transferred to a new tube, and washed once more. A centrifugation step (1 min at 720*g* and room temperature) separated unbound proteins from the resin after each wash. Bound proteins were eluted from the resin with 2× Tris-Tricine SDS−PAGE sample loading buffer and heated for 2 min at 55 °C. Samples were analyzed by 10% Tris-Tricine SDS−PAGE.

RESULTS

Two Products from One Gene. We expressed His-tagged YscQ recombinantly in *E. coli* and found that it was copurified as two protein products throughout Ni^{2+}-chelation and size-exclusion chromatography (Figure 1a). The first product migrated on SDS−PAGE at ∼36 kDa, the expected size for intact YscQ (307 residues) containing a C-terminal His tag, and the second migrated at ∼11 kDa. The larger product was verified to be intact YscQ by N-terminal sequencing, which also revealed that the ∼11 kDa product began at residue 218 and corresponded to the C-terminal portion of YscQ. While truncation fragments often arise because of inadvertent proteolysis, it was notable that residue 218 was a Met. This raised the possibility that the initiation of translation at codon 218 in *yscQ* had given rise to the C-terminal product, hereafter called YscQ-C (residues 218−307). Consistent with this hypothesis, a possible ribosome-binding site (RBS) upstream of codon 218 was found (Figure S1 of the Supporting Information).

To test whether an internal translation initiation site existed, M218 was substituted with Ala. Expression of YscQ(M218A) in *E. coli* yielded the ∼36 kDa intact YscQ product, but notably no YscQ-C (Figure 1b), providing evidence of an internal translation initiation site. We next purified endogenous YscQ from *Y. pseudotuberculosis* and detected both intact YscQ and

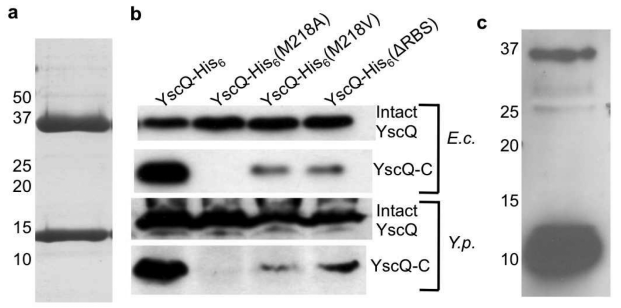

Figure 1. YscQ-C results from an internal translation initiation site. (a) YscQ expressed in *E. coli* and purified by Ni^{2+}-chelation and size-exclusion chromatography, as visualized by Coomassie-stained SDS−PAGE. Molecular mass markers are indicated at the left. Intact YscQ is the upper band at ∼36 kDa and YscQ-C the lower band at ∼11 kDa. (b) Wild-type and mutant YscQ expressed in *E. coli* (top two blots) and *Y. pseudotuberculosis* (bottom two) and detected by an anti-His Western blot from whole cell lysates. YscQ contains a C-terminal His tag and was detected as intact YscQ (top panel in each set) and YscQ-C (bottom panel in each set). (c) YscQ detected in *Y. pseudotuberculosis* by a Western blot using anti-YscQ polyclonal antibodies. Prior to the Western blot, YscQ was captured from a whole cell *Y. pseudotuberculosis* lysate by affinity chromatography using the same anti-YscQ polyclonal antibodies. Molecular mass markers are indicated at the left.

YscQ-C (Figure 1c). For this experiment, YscQ was captured and concentrated from a *Y. pseudotuberculosis* lysate using anti-YscQ polyclonal antibodies affixed to beads and detected by a Western blot using the same antibodies. These steps were necessary because the reactivity of the anti-YscQ polyclonal antibodies was poor. The imbalanced level of intact YscQ and YscQ-C was an artifact, as the same imbalance was observed through this procedure for YscQ expressed in *E. coli*, in which equivalent levels of YscQ and YscQ-C were known to be produced (Figure S2 of the Supporting Information). The imbalance may be due to the fact that the antibodies were raised against YscQ-C, which appears to differ in conformation from intact YscQ (see below).

Internal Translation Initiation Site. To overcome problems associated with the low sensitivity of our anti-YscQ polyclonal antibodies, we expressed His-tagged versions of YscQ in *Y. pseudotuberculosis* using the inducible *araBAD* promoter of the pBAD plasmid. As expected from the results with endogenous YscQ, His-tagged YscQ was expressed as two products in *Y. pseudotuberculosis*, intact YscQ and YscQ-C, as detected by an anti-His Western blot (Figure 1b). Notably, expression of YscQ(M218A) in *Y. pseudotuberculosis* resulted in only one product, intact YscQ. No YscQ-C was observed, as had been the case in *E. coli*.

We next substituted the ATG codon at position 218 with GTG, which encodes valine and can function as an alternative initiation codon in bacteria. This substitution, YscQ(M218V), resulted in two protein products, intact YscQ and YscQ-C, in both *Y. pseudotuberculosis* and *E. coli* (Figure 1b). GTG was less efficient than ATG as an initiation codon and yielded less YscQ-C than intact YscQ. We also created a silent mutation in the putative ribosome-binding site upstream of codon 218 (GGAGTT → AGAATT). This mutation, YscQ(ΔRBS), substantially diminished the efficiency of the internal translation initiation site in *Y. pseudotuberculosis* and *E. coli* (Figure 1b). In summary, these results provide strong evidence of the existence of an internal translation initiation site at codon 218, which

dx.doi.org/10.1021/bi201792p | *Biochemistry* 2012, 51, 1669−1677

results in two distinct proteins being produced from the single *yscQ* locus.

Structure of YscQ-C. YscQ-C was expressed in *E. coli*, purified, and crystallized. The 2.25 Å resolution limit structure of YscQ-C was determined by single-wavelength anomalous dispersion (Table 1). Except for the first 11 residues, which were presumably flexible, the entirety of YscQ-C was visible and unambiguously traced. The structure revealed a highly intertwined dimer (Figure 2a), characteristic of the SpoA fold

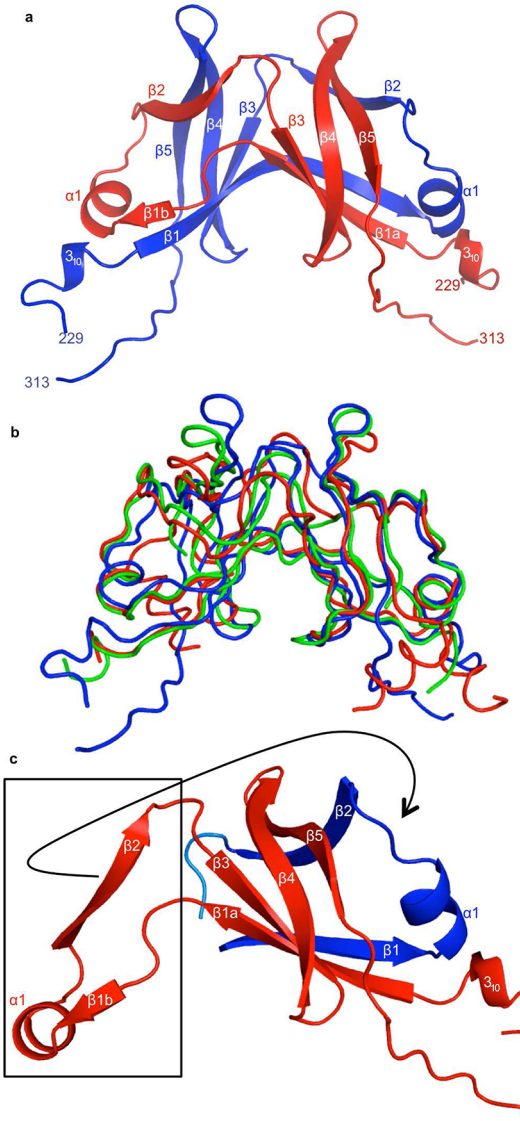

Figure 2. Structure of YscQ-C. (a) YscQ-C dimer in ribbon representation, with individual protomers colored red and blue. (b) Superposition of YscQ-C (blue), *T. maritima* FliN (red), and *P. syringae* $HrcQ_B$ (green) in coil representation. (c) The domain-swapped subdomain of YscQ-C is boxed. The subdomain could conceivably pivot at the disruption in strand $\beta1$ and the loop between $\beta2$ and $\beta3$ to form intramolecular contacts and replace the equivalent blue domain. This would result in a monomeric form of the YscQ-C domain.

in fragments of *T. maritima* FliN[8] (29% sequence identity, 3.2 Å rmsd, 75 Cα atoms, *Z* score of 7.4) and *P. syringae* $HrcQ_B$[22] (27% sequence identity, 2.3 Å rmsd, 70 Cα atoms, *Z* score of 7.4) (Figure 2b and Figure S3 of the Supporting Information). As in FliN and $HrcQ_B$, each YscQ-C protomer consists of five β-strands ($\beta1-\beta5$) with a short helix ($\alpha1$) between $\beta1$ and $\beta2$. The 10 antiparallel β-strands in the YscQ-C dimer assemble to form a saddle-shaped structure. The YscQ-C protomers are related by approximate 2-fold symmetry but are not identical (rmsd 1.4 Å, 85 Cα atoms), which is most apparent at strand $\beta1$ (Figure 2a). In one of the protomers, this β-strand is disrupted (between $\beta1$a and $\beta1$b) and several residues within this disruption have orientations opposite to those in the other protomer (Figure S3 of the Supporting Information). Each protomer buries ~2140 Å^2 of surface area at the largely apolar intermolecular interface (dominated by F242, W251, L262, V269, and L294). The identity of these residues is not conserved in FliN and $HrcQ_B$, but their hydrophobic nature is (Figure S4 of the Supporting Information). The same is true for T3S orthologs of YscQ (Figure S5 of the Supporting Information). The hydrophobic interactions in YscQ-C are supplemented by a large number of β-sheet hydrogen bonds between the antiparallel $\beta1$ strands. The surface of YscQ-C contains extensive patches of hydrophobic residues (Figure S6 of the Supporting Information), consistent with it being involved in protein−protein interactions as part of the putative C-ring. One of these patches occurs at the dyad axis of the homodimer (Figure S6b of the Supporting Information), at a location equivalent to one in FliN that has been shown to be functionally important in mediating interactions with the ATPase regulator FliH.[39]

The highly intertwined nature of the YscQ-C homodimer is caused by domain swapping. A subdomain that consists of part of strand $\beta1$ through strand $\beta2$ from one protomer (Figure 2c, boxed) reaches across and contacts the adjacent protomer. This same subdomain could conceivably reorient and snap back to contact the same protomer from which it originated (Figure 2c), thereby conferring a monomeric state to the SpoA domain, as has been suggested for FliM.[9] A reasonable hinge for this snap back occurs at the disruption in strand $\beta1$ in conjunction with the loop between strands $\beta2$ and $\beta3$.

Intact YscQ and YscQ-C Form a 1:2 Complex. The copurification of intact YscQ with YscQ-C suggested that they formed a complex. To test this hypothesis, we separately expressed and purified intact YscQ, as produced by YscQ-(M218A), and YscQ-C, and incubated the two proteins together. The resulting mixture ran on a gel filtration column at a position earlier than that of either YscQ(M218A) or YscQ-C (Figure 3a). Significantly, this distinct and shifted position coincided precisely with the position of YscQ purified from *E. coli*, which consists of both intact YscQ and YscQ-C. These results confirm that YscQ and YscQ-C interact to form a complex and show that the complex can be reconstituted from individual components. The YscQ−YscQ-C complex was determined to have a molecular mass of 52.8 kDa by static light scattering (Figure 3b). This corresponds to a single molecule of intact YscQ (35.0 kDa calculated) bound to a homodimer of YscQ-C (21.5 kDa calculated). The homodimeric nature of YscQ-C, as observed in the crystal structure, was confirmed by static light scattering (19.8 kDa measured) (Figure 3b). Such measurements were difficult with YscQ-(M218A) because of high-molecular mass impurities. However, we note that YscQ(M218A) ran between the YscQ−YscQ-C complex and YscQ-C on the gel filtration column (Figure 3a), indicative of a monomeric state for YscQ(M218A).

The 1:2 stoichiometry of the YscQ−YscQ-C complex leads to the conclusion that the sequence-identical SpoA domains of intact YscQ and YscQ-C take on different conformations. To

dx.doi.org/10.1021/bi201792p | *Biochemistry* 2012, 51, 1669−1677

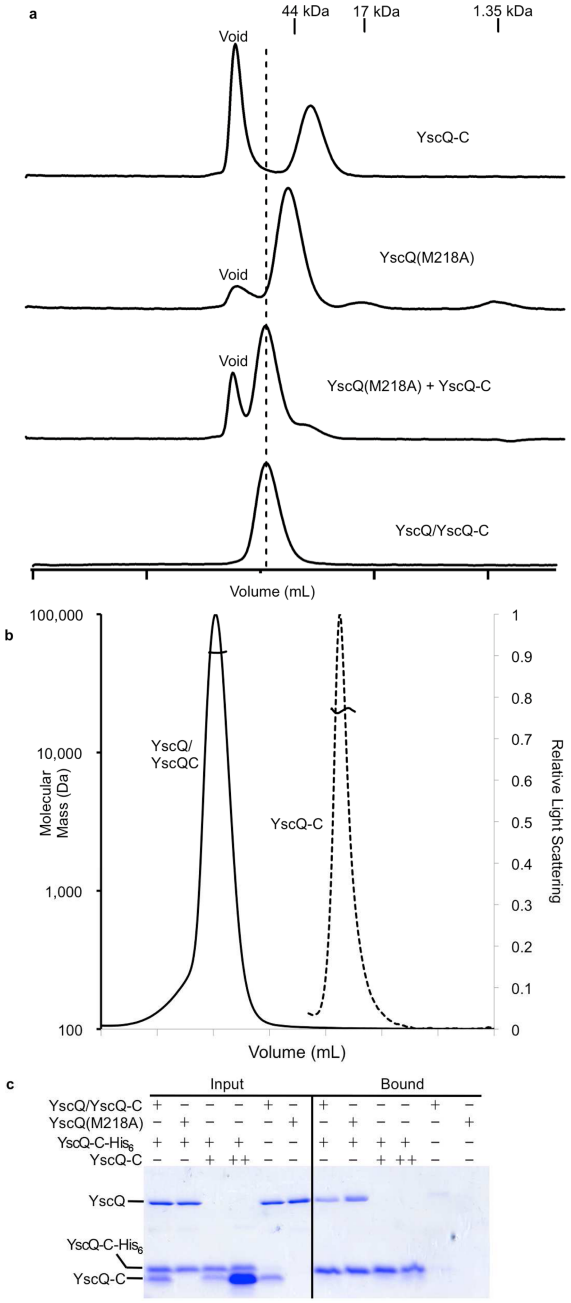

Figure 3. Intact YscQ and YscQ-C form a 1:2 heterotrimer. (a) Gel filtration chromatographic profiles of YscQ-C, YscQ(M218A), YscQ-(M218A) incubated with YscQ-C, and YscQ purified from *E. coli* (YscQ–YscQ-C). (b) Static light scattering of the YscQ–YscQ-C complex and YscQ-C applied to a gel filtration column. The molar mass is indicated across the peaks. The proteins were run separately, but the chromatograms were superimposed for display purposes. (c) Exchangeability of the YscQ–YscQ-C complex and YscQ-C evaluated by incubating YscQ-C-His_6 separately with the untagged YscQ–YscQ-C complex, YscQ(M218A), and YscQ-C. Association was detected by Ni^{2+}-NTA coprecipitation and visualized by Coomassie-stained Tris-Tricine SDS–PAGE.

test this unusual conclusion, we examined the exchangeability of components in the 1:2 YscQ–YscQ-C complex. We first confirmed that YscQ-C forms a nonexchangeable homodimer, as suggested by its extensive intermolecular interface. To do this, we incubated His-tagged YscQ-C with untagged YscQ-C and observed no exchange of partners in a Ni^{2+}-NTA coprecipitation assay, even with an excess of untagged YscQ-C (Figure 3c). We next confirmed that intact YscQ, in the form of YscQ(M218A), associates with YscQ-C by incubating the two proteins together and observing the coprecipitation of YscQ(M218A) with His-tagged YscQ-C. We then asked whether free His-tagged YscQ-C would exchange with untagged YscQ-C from the YscQ–YscQ-C complex. We reasoned that if the SpoA domain in intact YscQ interacted with the SpoA domain in YscQ-C through the domain swap observed for YscQ-C, then no exchange should occur. We instead found that a portion of the YscQ–YscQ-C complex had acquired His-tagged YscQ-C, providing evidence of exchange. These data indicate that the SpoA domain in intact YscQ does not engage in the irreversible, dimeric intertwining seen in YscQ-C but instead takes on a different conformation.

Both Intact YscQ and YscQ-C Are Required for Type III Secretion. We last examined the significance of the internal initiation site for type III secretion. We constructed an in-frame *yscQ* deletion mutant in *Y. pseudotuberculosis* and showed that, as expected,[13] the loss of YscQ abrogated type III secretion (Figure 4, Δ*yscQ*). The deletion was nonpolar, as type III

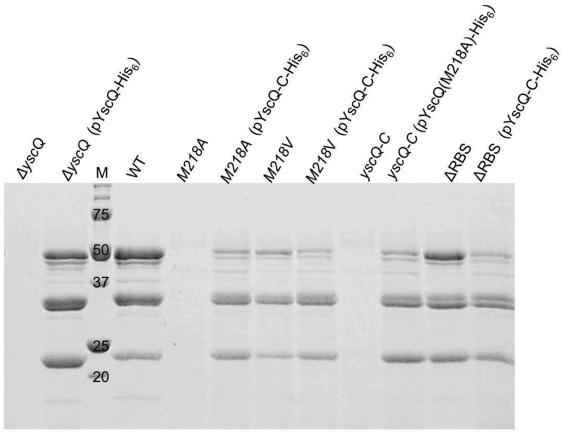

Figure 4. Both intact YscQ and YscQ-C are required for T3S. Proteins secreted via the T3S system by *Y. pseudotuberculosis* expressing wild-type (WT) or various mutant alleles of *yscQ* were detected by Coomassie-stained SDS–PAGE. Mutant alleles were incorporated into the native locus on the pYV plasmid by allelic exchange or expressed ectopically from the pBAD plasmid (designated by parentheses). Lane M contained molecular mass markers (kilodaltons).

secretion was restored by complementation with wild-type, His-tagged YscQ expressed from pBAD (Figure 4). Next, various alleles of *yscQ* were introduced by allelic exchange into their native locus on the pYV virulence plasmid of *Y. pseudotuberculosis*, and the resulting strains were tested for type III secretion. Notably, we found that *Y. pseudotuberculosis* expressing either the *yscQ*-M218A allele or the *yscQ*-C allele (encoding just residues 218–307) was deficient in type III secretion (Figure 4). Type III secretion was restored in these strains by expressing YscQ-C or YscQ(M218), respectively, from a plasmid. These results indicate that the YscQ–YscQ-C complex is required for T3S, and that the internal translation initiation site is essential for function. It should be noted that the slight differences among samples in quantities of proteins secreted were not significant, as these were representative of the typical variability in the procedure. No defect in type III secretion was seen for either the *yscQ*-M218V allele or the RBS mutated allele, and no effect was seen when additional YscQ-C was

dx.doi.org/10.1021/bi201792p | *Biochemistry* 2012, 51, 1669–1677

expressed from a plasmid in these strains. This means that an imbalanced ratio of intact YscQ relative to YscQ-C is not detrimental and suggests that YscQ is produced in excess in *Y. pseudotuberculosis*.

DISCUSSION

Type III secretion systems generally encode a single protein in place of the two flagellar proteins FliM and FliN, which associate to form the flagellar C-ring. These T3S cognates are similar in their N-terminal domains to FliM and are as large as FliM but more closely resemble FliN in their C-terminal SpoA domains. Most T3S systems appear to lack a smaller FliN-sized cognate to accompany the larger FliM-sized cognate. We have discovered that in the *Yersinia* T3S system, a FliN-sized cognate exists. The FliN-sized cognate, YscQ-C, is not encoded by a separate locus but is instead produced by an internal translation initiation site within the locus encoding the FliM-sized cognate YscQ. This is similar to a recently described case in the *Salmonella* SPI-2 T3S system for the YscQ ortholog SsaQ.[16] A C-terminal fragment of SsaQ, called $SsaQ_s$, arises from an internal translation start site, and this fragment associates with intact SsaQ. However, the mechanisms of action of $SsaQ_s$ and YscQ-C differ considerably. In contrast to the essential nature of YscQ-C for T3S in *Yersinia*, $SsaQ_s$ was found to be dispensable for T3S in *Salmonella*.[16] In the absence of $SsaQ_s$, proteins are still secreted by the T3S system, albeit at a somewhat diminished level.[16] Notably, this diminution was observed to be complemented by overexpression of intact SsaQ. The dispensability of $SsaQ_s$ is explained by the fact that $SsaQ_s$, rather than acting as a part of the T3S apparatus, is a chaperone for intact SsaQ, as evidenced by the fact that intact SsaQ has a shorter intrabacterial half-life in the absence of $SsaQ_s$.[16] This chaperone mode of action for $SsaQ_s$ is unusual and unprecedented for FliN family members. In contrast, our evidence suggests that YscQ-C mimics FliN in forming an essential part of the T3S system.

The internal translation start site in SsaQ is at a slightly different location relative to the one in YscQ (Figure S5 of the Supporting Information). However, the N-terminus of YscQ-C is disordered, and thus, the exact location of the start site is unlikely to be consequential. An examination of other YscQ orthologs reveals that the M218 internal translation initiation site is precisely conserved in *Pseudomonas aeruginosa* PscQ, *Aeromonas hydrophila* AscQ, *Photorhabdus luminescens* LscQ, and *Arsenophonus nasoniae* SctQ (Figure S5 of the Supporting Information). In each of these cases, a potential ribosome binding site also exists upstream of the Met codon (Figure S1 of the Supporting Information). This pattern of conservation indicates that these YscQ orthologs are also likely to produce FliN cognates through an internal translation initiation site. However, M218 is not conserved in all YscQ orthologs. For example, *Shigella* Spa33, *Salmonella* SpaO (from the SPI-1 T3S system), and *E. coli* EscQ (SepQ) lack the equivalent of M218. They also do not have nearby ATG codons. Bacteria can also use TTG, GTG, and CTG as start codons, and while these exist near the equivalent of M218, it is impossible to say with confidence that these are used as internal translation initiation sites because of the absence of unambiguous ribosome binding sites upstream of these codons. It is possible that in these latter cases an alternative mechanism (e.g., proteolysis) exists to generate a FliN-sized cognate or that the putative T3S C-ring functions without one.

We determined that intact YscQ and YscQ-C associate to form a complex. Likewise, $HrcQ_B$ interacts directly with the FliM-sized cognate $HrcQ_A$,[22] and $SsaQ_s$ interacts either directly or indirectly with the FliM cognate SsaQ;[16] however, the stoichiometries of these associations are unknown. We determined the stoichiometry of the YscQ–YscQ-C complex to be 1:2, which is similar to the value of 1:4 reported for the FliM–FliN complex in having a single large component bound to several smaller ones but of course differs in the number of smaller ones.[8] The FliN tetramer appears to consist of either an extended or donut-shaped dimer of dimers.[22,40,41] The residues that mediate the dimer-of-dimer contacts, however, are not conserved in YscQ (Figure S4 of the Supporting Information), and no evidence of tetramerization of YscQ-C was found in solution or in the crystal. Interactions between FliM and FliN are mediated by their SpoA domains.[10] While the SpoA domain in FliN confers homodimerization,[8] the one in FliM does not. Instead, the SpoA domain in FliM forms an uncharacterized structure that supports association with FliN homodimers.[9] Our observations with YscQ are consistent with these conclusions but extend them by one step, as the SpoA domains in FliM and FliN are only similar in sequence while those in intact YscQ and YscQ-C are exactly identical.

The SpoA domain of YscQ-C, as indicated by its crystal structure, exists as a domain-swapped homodimer. Consistent with its highly intertwined structure, YscQ-C was found to exist as a stable dimer and dissociate only upon denaturation. The structure of the SpoA domain in intact YscQ is unknown. However, the monomeric nature of intact YscQ and its exchangeability indicate that the SpoA domain in intact YscQ takes on a conformation different from the one in YscQ-C. We suggest that the N-terminal portions of YscQ disfavor the intermolecular, domain-swapped interactions of the SpoA domain seen in YscQ-C and instead favor intramolecular, nonswapped interactions within the SpoA domain (Figure 5).

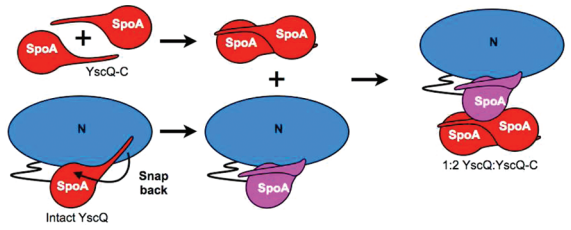

Figure 5. Schematic of the assembly of the 1:2 intact YscQ–YscQ-C complex. The SpoA domain of YscQ-C, in the absence of the N-terminal domain (N) of YscQ, takes on a domain-swapped homodimeric conformation (red). In contrast, in the presence of the N-terminal domain, the SpoA domain is unable to form a domain-swapped homodimer and instead forms intramolecular contacts (purple). On the basis of analogy with the FliM–FliN complex, we also suggest that the monomeric, nonswapped SpoA domain in intact YscQ mediates association with the domain-swapped SpoA domains in the YscQ-C homodimer, resulting in the 1:2 intact YscQ–YscQ-C complex.

More specifically, we suggest that the N-terminal regions contact the SpoA domain, perhaps at the suggested snap-back hinge (i.e., disruption in strand β1 along with the loop between strands β2 and β3), to favor these interactions. It is worth noting that the sequence at the disruption in strand β1 is conserved among YscQ orthologs. In analogy with the FliM–FliN and the $HrcQ_A$–$HrcQ_B$ complexes,[10,22] the nonswapped

dx.doi.org/10.1021/bi201792p | *Biochemistry* 2012, 51, 1669–1677

SpoA domain of intact YscQ is likely to mediate interactions with the domain-swapped SpoA domain of the YscQ-C homodimer.

In summary, we have identified an essential internal translation initiation site in *yscQ*. This site is necessary for the synthesis of YscQ-C, a functionally required component of the 1:2 YscQ−YscQ-C complex, which is a close mimic of the 1:4 FliM−FliN complex and is the likely fundamental building block of the putative C-ring in *Yersinia*.

■ ASSOCIATED CONTENT

Supporting Information

Figures S1−S6. This material is available free of charge via the Internet at http://pubs.acs.org.

■ AUTHOR INFORMATION

Corresponding Author

*Phone: (858) 822-1139. Fax: (858) 822-2871. E-mail: pghosh@ucsd.edu.

Present Address

[†]Department of Molecular Medicine, City of Hope Beckman Research Institute, 1500 E. Duarte Rd., Duarte, CA 91010.

Funding

This work was supported by National Institutes of Health Grants T32 CA009523 (B.Y.H.) and R01 AI061452 (P.G.).

Notes

The authors declare no competing financial interest.

■ ACKNOWLEDGMENTS

We thank the staff at beamline 23 ID-B for help in data collection and Johanne Le Coq, Alicia Gamez, and other members of the Ghosh lab for helpful suggestions.

■ ABBREVIATIONS

2ME, 2-mercaptoethanol; RBS, ribosome-binding site; rmsd, root-mean-square deviation; SeMet, selenomethionine; SLS, static light scattering; T3S, type III secretion.

■ REFERENCES

(1) Galan, J. E., and Wolf-Watz, H. (2006) Protein delivery into eukaryotic cells by type III secretion machines. *Nature 444*, 567−573.

(2) Cornelis, G. R. (2006) The type III secretion injectisome. *Nat. Rev. Microbiol. 4*, 811−825.

(3) Kubori, T., Matsushima, Y., Nakamura, D., Uralil, J., Lara-Tejero, M., Sukhan, A., Galan, J. E., and Aizawa, S. I. (1998) Supramolecular structure of the *Salmonella typhimurium* type III protein secretion system. *Science 280*, 602−605.

(4) Akopyan, K., Edgren, T., Wang-Edgren, H., Rosqvist, R., Fahlgren, A., Wolf-Watz, H., and Fallman, M. (2011) Translocation of surface-localized effectors in type III secretion. *Proc. Natl. Acad. Sci. U.S.A. 108*, 1639−1644.

(5) Ghosh, P. (2004) Process of protein transport by the type III secretion system. *Microbiol. Mol. Biol. Rev. 68*, 771−795.

(6) Thomas, D. R., Francis, N. R., Xu, C., and DeRosier, D. J. (2006) The three-dimensional structure of the flagellar rotor from a clockwise-locked mutant of *Salmonella enterica* serovar *Typhimurium*. *J. Bacteriol. 188*, 7039−7048.

(7) Erhardt, M., and Hughes, K. T. (2010) C-ring requirement in flagellar type III secretion is bypassed by FlhDC upregulation. *Mol. Microbiol. 75*, 376−393.

(8) Brown, P. N., Mathews, M. A., Joss, L. A., Hill, C. P., and Blair, D. F. (2005) Crystal structure of the flagellar rotor protein FliN from *Thermotoga maritima*. *J. Bacteriol. 187*, 2890−2902.

(9) Sarkar, M. K., Paul, K., and Blair, D. F. (2010) Subunit organization and reversal-associated movements in the flagellar switch of *Escherichia coli*. *J. Biol. Chem. 285*, 675−684.

(10) Mathews, M. A., Tang, H. L., and Blair, D. F. (1998) Domain analysis of the FliM protein of *Escherichia coli*. *J. Bacteriol. 180*, 5580−5590.

(11) Diepold, A., Amstutz, M., Abel, S., Sorg, I., Jenal, U., and Cornelis, G. R. (2010) Deciphering the assembly of the *Yersinia* type III secretion injectisome. *EMBO J. 29*, 1928−1940.

(12) Morita-Ishihara, T., Ogawa, M., Sagara, H., Yoshida, M., Katayama, E., and Sasakawa, C. (2006) *Shigella* Spa33 is an essential C-ring component of type III secretion machinery. *J. Biol. Chem. 281*, 599−607.

(13) Fields, K. A., Plano, G. V., and Straley, S. C. (1994) A low-Ca^{2+} response (LCR) secretion (ysc) locus lies within the lcrB region of the LCR plasmid in *Yersinia pestis*. *J. Bacteriol. 176*, 569−579.

(14) Lara-Tejero, M., Kato, J., Wagner, S., Liu, X., and Galan, J. E. (2011) A sorting platform determines the order of protein secretion in bacterial type III systems. *Science 331*, 1188−1191.

(15) Biemans-Oldehinkel, E., Sal-Man, N., Deng, W., Foster, L. J., and Finlay, B. B. (2011) Quantitative Proteomic Analysis Reveals Formation of an EscL-EscQ-EscN Type III Complex in Enteropathogenic *Escherichia coli*. *J. Bacteriol. 193*, 5514−5519.

(16) Yu, X. J., Liu, M., Matthews, S., and Holden, D. W. (2011) Tandem Translation Generates a Chaperone for the *Salmonella* Type III Secretion System Protein SsaQ. *J. Biol. Chem. 286*, 36098−36107.

(17) Jackson, M. W., and Plano, G. V. (2000) Interactions between type III secretion apparatus components from *Yersinia pestis* detected using the yeast two-hybrid system. *FEMS Microbiol. Lett. 186*, 85−90.

(18) Blaylock, B., Riordan, K. E., Missiakas, D. M., and Schneewind, O. (2006) Characterization of the *Yersinia enterocolitica* type III secretion ATPase YscN and its regulator, YscL. *J. Bacteriol. 188*, 3525−3534.

(19) Riordan, K. E., Sorg, J. A., Berube, B. J., and Schneewind, O. (2008) Impassable YscP substrates and their impact on the *Yersinia enterocolitica* type III secretion pathway. *J. Bacteriol. 190*, 6204−6216.

(20) Johnson, D. L., Stone, C. B., and Mahony, J. B. (2008) Interactions between CdsD, CdsQ, and CdsL, three putative *Chlamydophila pneumoniae* type III secretion proteins. *J. Bacteriol. 190*, 2972−2980.

(21) Spaeth, K. E., Chen, Y. S., and Valdivia, R. H. (2009) The *Chlamydia* type III secretion system C-ring engages a chaperone-effector protein complex. *PLoS Pathog. 5*, e1000579.

(22) Fadouloglou, V. E., Tampakaki, A. P., Glykos, N. M., Bastaki, M. N., Hadden, J. M., Phillips, S. E., Panopoulos, N. J., and Kokkinidis, M. (2004) Structure of $HrcQ_B$-C, a conserved component of the bacterial type III secretion systems. *Proc. Natl. Acad. Sci. U.S.A. 101*, 70−75.

(23) Bolin, I., Norlander, L., and Wolf-Watz, H. (1982) Temperature-inducible outer membrane protein of *Yersinia pseudotuberculosis* and *Yersinia enterocolitica* is associated with the virulence plasmid. *Infect. Immun. 37*, 506−512.

(24) Budisa, N., Karnbrock, W., Steinbacher, S., Humm, A., Prade, L., Neuefeind, T., Moroder, L., and Huber, R. (1997) Bioincorporation of telluromethionine into proteins: A promising new approach for X-ray structure analysis of proteins. *J. Mol. Biol. 270*, 616−623.

(25) Kabsch, W. (2010) XDS. *Acta Crystallogr. D66*, 125−132.

(26) Otwinowski, Z., and Minor, W. (1997) *Processing of X-ray Diffraction Data Collected in Oscillation Mode*, Vol. *276*, Academic Press, New York.

(27) Adams, P. D., Afonine, P. V., Bunkoczi, G., Chen, V. B., Davis, I. W., Echols, N., Headd, J. J., Hung, L. W., Kapral, G. J., Grosse-Kunstleve, R. W., McCoy, A. J., Moriarty, N. W., Oeffner, R., Read, R. J., Richardson, D. C., Richardson, J. S., Terwilliger, T. C., and Zwart, P. H. (2010) PHENIX: A comprehensive Python-based system for macromolecular structure solution. *Acta Crystallogr. D66*, 213−221.

(28) Emsley, P., and Cowtan, K. (2004) Coot: Model-building tools for molecular graphics. *Acta Crystallogr. D60*, 2126−2132.

(29) Brünger, A. (1998) Crystallography & NMR system: A new software for macromolecular structure determination. *Acta Crystallogr. D54*, 905−921.
(30) Winn, M. D., Ballard, C. C., Cowtan, K. D., Dodson, E. J., Emsley, P., Evans, P. R., Keegan, R. M., Krissinel, E. B., Leslie, A. G., McCoy, A., McNicholas, S. J., Murshudov, G. N., Pannu, N. S., Potterton, E. A., Powell, H. R., Read, R. J., Vagin, A., and Wilson, K. S. (2011) Overview of the CCP4 suite and current developments. *Acta Crystallogr. D67*, 235−242.
(31) Winn, M. D., Isupov, M. N., and Murshudov, G. N. (2001) Use of TLS parameters to model anisotropic displacements in macromolecular refinement. *Acta Crystallogr. D57*, 122−133.
(32) Chen, V. B., Arendall, W. B. III, Headd, J. J., Keedy, D. A., Immormino, R. M., Kapral, G. J., Murray, L. W., Richardson, J. S., and Richardson, D. C. (2010) MolProbity: All-atom structure validation for macromolecular crystallography. *Acta Crystallogr. D66*, 12−21.
(33) Di Tommaso, P., Moretti, S., Xenarios, I., Orobitg, M., Montanyola, A., Chang, J. M., Taly, J. F., and Notredame, C. (2011) T-Coffee: A web server for the multiple sequence alignment of protein and RNA sequences using structural information and homology extension. *Nucleic Acids Res. 39*, W13−W17.
(34) Gouet, P., Robert, X., and Courcelle, E. (2003) ESPript/ENDscript: Extracting and rendering sequence and 3D information from atomic structures of proteins. *Nucleic Acids Res. 31*, 3320−3323.
(35) Lathem, W. W., Price, P. A., Miller, V. L., and Goldman, W. E. (2007) A plasminogen-activating protease specifically controls the development of primary pneumonic plague. *Science 315*, 509−513.
(36) Datsenko, K. A., and Wanner, B. L. (2000) One-step inactivation of chromosomal genes in *Escherichia coli* K-12 using PCR products. *Proc. Natl. Acad. Sci. U.S.A. 97*, 6640−6645.
(37) Palmer, L. E., Hobbie, S., Galan, J. E., and Bliska, J. B. (1998) YopJ of *Yersinia pseudotuberculosis* is required for the inhibition of macrophage TNF-α production and downregulation of the MAP kinases p38 and JNK. *Mol. Microbiol. 27*, 953−965.
(38) Rodgers, L., Mukerjea, R., Birtalan, S., Friedberg, D., and Ghosh, P. (2010) A solvent-exposed patch in chaperone-bound YopE is required for translocation by the type III secretion system. *J. Bacteriol. 192*, 3114−3122.
(39) Paul, K., Harmon, J. G., and Blair, D. F. (2006) Mutational analysis of the flagellar rotor protein FliN: Identification of surfaces important for flagellar assembly and switching. *J. Bacteriol. 188*, 5240−5248.
(40) Fadouloglou, V. E., Bastaki, M. N., Ashcroft, A. E., Phillips, S. E., Panopoulos, N. J., Glykos, N. M., and Kokkinidis, M. (2009) On the quaternary association of the type III secretion system HrcQB-C protein: Experimental evidence differentiates among the various oligomerization models. *J. Struct. Biol. 166*, 214−225.
(41) Paul, K., and Blair, D. F. (2006) Organization of FliN subunits in the flagellar motor of *Escherichia coli*. *J. Bacteriol. 188*, 2502−2511.